Experimental Investigation of Load Sharing in Multiple Gear Tooth Contact Using the Stress-Optical Method of Caustics

V. Spitas*, G. A. Papadopoulos†, C. Spitas* and T. Costopoulos†

*Technical University of Crete, GR-73100, Akrotiri, Chania, Greece

†National Technical University of Athens, GR-157 73, Zografou, Athens, Greece

ABSTRACT: In this paper, a comprehensive methodology for calculating load sharing in multiple tooth contact is presented based on the experimental stress-optical method of caustics. The technique is applied to a set of poly-methyl-methacrylate gears at various meshing positions covering a complete meshing cycle, including single and multiple gear tooth contact. The load sharing factor (LSF) is calculated using well-established mathematical formulae from the photographs of the transmitted caustics and the obtained results are compared with the pertinent International Organisation for Standardisation and American Gear Manufacturers Association standards with which good agreement is verified. The proposed method is a reliable alternative for measuring load distribution in gear teeth compared with photoelasticity and other experimental techniques.

KEY WORDS: *caustics, contact, experimental method, gears, load-sharing*

NOTATION

c_t	Stress-optical constant	t	Specimen thickness
D_x	Maximum diameter of caustic	X_t, Y_t	Coordinates of caustic
E	Young's modulus	z	Number of teeth
LSF	Load-sharing factor	z_i	Distance between focal point and specimen
l	Contact half-length	z_o	Distance between screen and specimen
m	Gear module	θ	Maximum meshing angle
P	Normal load per unit width	θ_{LPSTC}	LPSTC meshing angle
P_i	Normal load on tooth i	θ_{HPSTC}	HPSTC meshing angle
$p(s)$	Contact pressure distribution	λ_{m}	Magnification
R	Equivalent radius of curvature	v	Poisson's ratio
$R_{1,2}$	Radii of curvature of bodies 1, 2	ω	Meshing angle

Introduction

In every working gear pair, the gear teeth deform elastically under the mesh forces. This deformation leads to angular displacements of the meshing gears commonly referred to as 'transmission errors (TE)'. These errors, which are not constant with time, are known to induce vibration and noise in gear drives and are frequently responsible for reduced fatigue life. All techniques aiming to lower the vibration concentrate on obtaining more progressive tooth engagement or, in other words, on improving load sharing between multiple gear tooth contact (Liou *et al.* [1], Munro [2], Spitas *et al.* [3]).

In order to estimate the load sharing between the meshing tooth pairs, several different approaches have been proposed. Early studies (Cornell [4]) usually employed simplified models for the gear tooth geometry and estimated tooth compliances analytically, which, however, due to the linearisation of the Hertzian compliance, introduced significant errors in the overall estimation of the load-sharing factor (LSF). Numerical analysis of multiple-contact gear tooth models is widely used today (Gosselin *et al.* [5], Zhang and Fang [6], Aziz *et al.* [7]) to simulate tooth contact and to calculate load sharing for different gear geometries.

Regarding the experimental assessment of gear tooth-loading conditions, several problems appear, rendering the use of classical methods of experimental stress analysis (i.e. strain gauges and extensometers) problematic, mainly because of the small

physical size of gear teeth and the even smaller dimensions of the highly loaded regions, i.e. contact points, critical sections, etc. Photoelasticity has been widely used for the experimental stress analysis of gears, particularly, because it offers a convenient way of assessing the maximum stress at the tooth root fillet (Lingaiah and Ramachandra [8], Deuschle *et al.* [9], Wang [10], Novikov *et al.* [11], Spitas *et al.* [12], Spitas and Spitas [13]). Although popular, photoelasticity is practically impossible to use in high stress concentration regions such as contact points and crack tips because of the very high density of the isochromatic fringes near the point of stress singularity. Other non-stress optical methods for the direct measurement of contact stresses such as the use of ultrasounds (Quinn *et al.* [14]), which measure the contact pressure from the variation of the ultrasonic reflection coefficient with respect to the dimensions of the actual contact area, have provided ambiguous results when compared with numerical predictions.

In this paper, the stress-optical method of caustics (Manogg [15], Theocaris [16], Theocaris and Gdoutos [17], Kalthoff [18], Papadopoulos [19]) is used for the first time to measure the contact load of gear tooth pairs in mesh. The maximum diameter of the transmitted caustic is mathematically linked to the length of the bearing contact and hence the bearing load. A special test rig has been designed and constructed at the Laboratory of Machine Elements of the National Technical University of Athens (NTUA) for testing multi-tooth gear models and the infrastructure of the Laboratory of Strength of Materials of NTUA has been used to perform the caustics measurements. The experimental findings are compared with the prevailing gear standards International Organisation for Standardisation (ISO) 6336 [20] and ANSI American Gear Manufacturers Association (AGMA) B88 [21].

Application of the Stress-Optical Method of Caustics for Measurement of Contact Load

In gear tooth contact, the individual teeth in mesh can be treated as a pair of perfectly elastic bodies, 1 and 2, each with a local curvature of R_1 and R_2, respectively, subjected to a normal load per unit width equal to P as in Figure 1. Assuming a contact width equal to $2l$, the Hertzian pressure distribution is (Johnson [22]):

$$p(s) = p_{\max}\sqrt{1-\left(\frac{s}{l}\right)^2} \quad \text{for } s = -l \rightarrow +l \tag{1}$$

The half-width l of the contact area is liked to the applied load through the relation [22]:

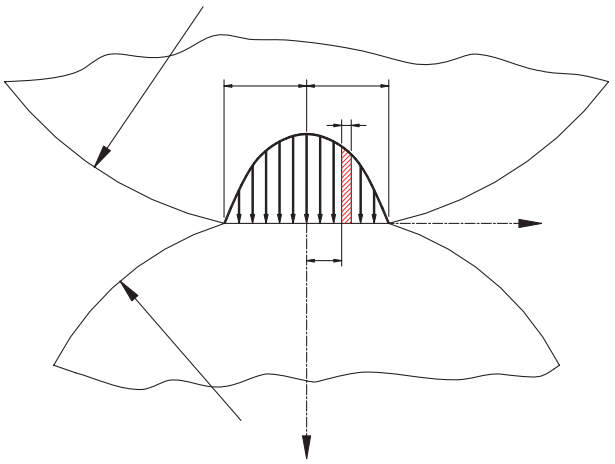

Figure 1: Hertzian stress distribution between two elastic bodies in contact

$$l = \sqrt{\frac{2kRP}{\pi}} \tag{2}$$

where $k = (1 - \nu^2)/\pi E$, assuming the same Young's modulus and Poisson's ratio for the bodies in contact, $R = R_1R_2/(R_1 + R_2)$ is the equivalent radius of curvature and

$$P = \int_{-l}^{l} p(s)\mathrm{d}s$$

is the applied load per unit width.

The experimental set-up for obtaining caustics from a transparent test specimen with contact stress singularities is illustrated in Figure 2. The light beam of a laser passes through a special filter and two convergent lenses, to become a convergent beam. In front of and behind the specimen, screens are placed at distances z_o parallel to the mid-plane of the specimen. From the reflected and transmitted (in case of transparent specimen) light rays from the specimen interference fringes (caustics) are formed on the screens. Because of the divergent light beam, the produced caustics are magnified by a specific factor λ_{m}, given by the relation [19]:

$$\lambda_{\mathrm{m}} = \frac{z_o + z_i}{z_i} \tag{3}$$

where z_o is the distance between the mid-plane of the specimen and the screen and z_i is the distance between the focal point and the mid-plane of the specimen.

Using the theory of caustics [15–19, 23–24], it is possible to correlate the maximum diameter D_x of the transmitted caustic with the contact length $2l$ by numerically solving the following system of equations:

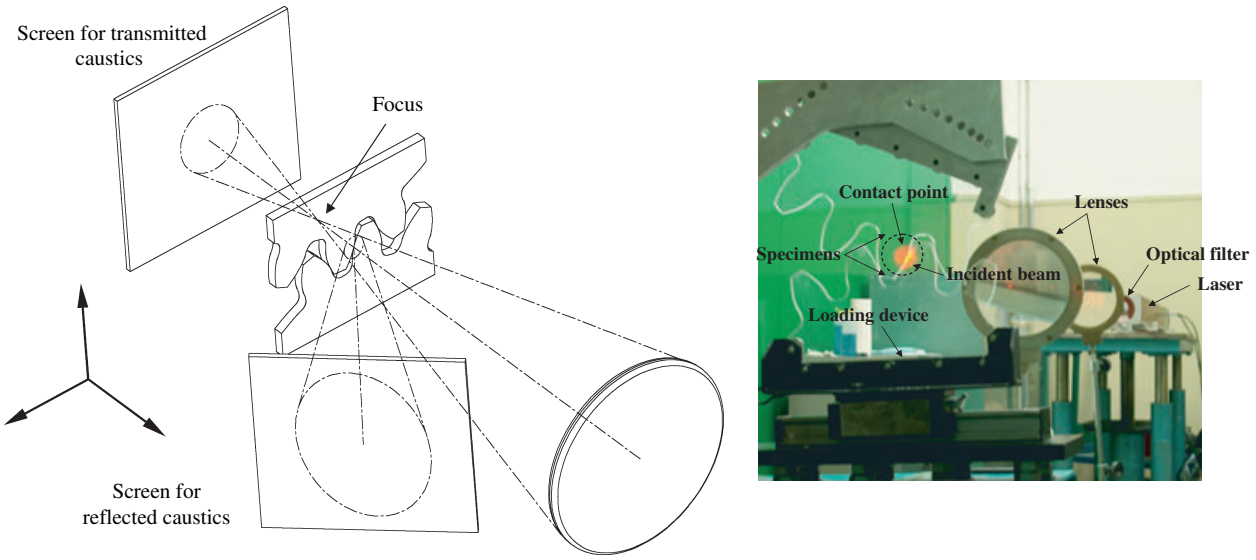

Figure 2: Schematic and actual experimental caustics layout

$$D_x = 2r\lambda_m\left(\cos\theta + \frac{g}{2}\sin 2\theta\right) \tag{4}$$

$$\theta = \sin^{-1}\left[\frac{\sqrt{1+8g^2}-1}{4g}\right] \tag{5}$$

$$g = \frac{C_t^{**}l^2}{r^3} \tag{6}$$

Knowing the contact length $2l$, the total load P can be computed through Equation (2).

Load-Sharing Calculation as per AGMA and ISO Standards

In gears with contact ratios lower than 2, which represent the majority of geared power transmissions based on the 20° involute system, contact takes place either between a single pair of teeth or two pairs of teeth. In the latter case, the total transmitted load is shared between the meshing tooth pairs and this is quantified by means of a non-dimensional factor termed 'load-sharing factor' (LSF) given by the equation:

$$\text{LSF} = \frac{P_i}{P} \tag{7}$$

where P_i is the load carried by the pair and P the total load along the path of contact. The LSF is dependent on tooth compliance, which in turn is a function of gear position and load, and is hence a nonlinear quantity.

Referring to Figure 3, a tooth pair load cycle can be described as follows:

Step 1. A new tooth pair (shaded teeth) engages in such a manner that the root of the driving gear contacts the tip of the driven gear. This position is herein set as $\omega = 0$. As can be seen in Figure 3A, two pairs of teeth are simultaneously engaged after this position.

Step 2. At position $\omega = \theta_{\text{LPSTC}}$ (Figure 3B) the previous pair disengages, and single-tooth contact commences. This condition defines the lowest point of single tooth contact (LPSTC) on the engaged tooth of the driving gear.

Step 3. At position $\omega = \theta_{\text{HPSTC}}$ (Figure 3C) the next tooth pair engages, so that double tooth contact is resumed. This condition defines the highest point of single tooth contact (HPSTC) on the engaged tooth of the driving gear.

Step 4. The load cycle ends at $\omega = \theta$ (where θ is the total meshing angle), at which point the tooth pair disengages as the tip of the driving gear contacts the root of the driven gear.

The meshing cycle described in steps 1–4 is characterised by double tooth contact at the intervals $0 < \omega < \theta_{\text{LPSTC}}$ and $\theta_{\text{HPSTC}} < \omega < \theta$ and single tooth contact at the interval $\theta_{\text{LPSTC}} < \omega < \theta_{\text{HPSTC}}$. The cycle repeats itself periodically for each new engaging tooth pair, dictating a similar behaviour for the LSF.

The prevailing AGMA standard (AGMA B88 [21]) for calculating the rating factors of spur and helical gear performance proposes a simplified approach to the above problem. According to this standard, as the gear pair passes from double tooth contact at the beginning of its meshing cycle, to single tooth contact at the LPSTC and to double tooth contact again

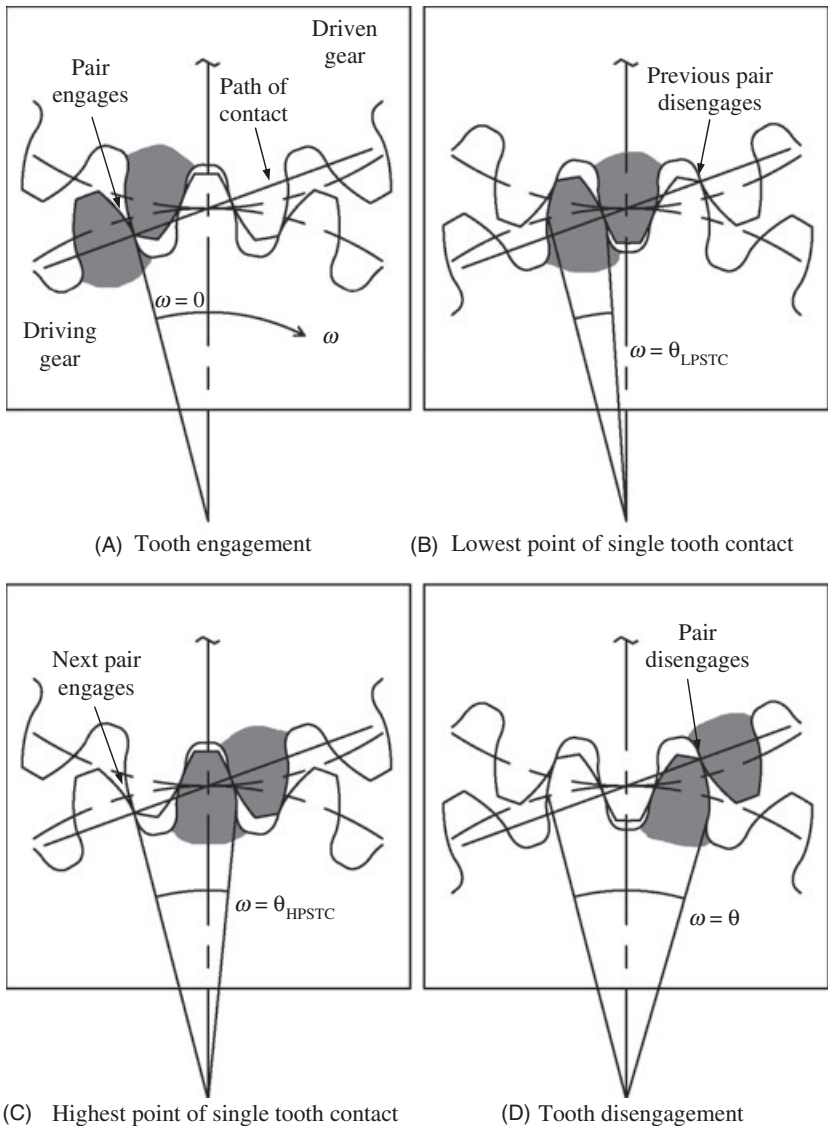

Figure 3A–D: Definition of meshing angle at various engagement positions

at the HPSTC, the LSF changes linearly following the relationship:

$$\mathrm{LSF}(\omega) = \frac{1}{3} + \frac{1}{3}\frac{\omega}{\theta_{\mathrm{LPSTC}}} \quad \text{for } 0 \le \omega < \theta_{\mathrm{LPSTC}} \tag{8}$$

$$\mathrm{LSF}(\omega) = 1 \quad \text{for } \theta_{\mathrm{LPSTC}} \le \omega \le \theta_{\mathrm{HPSTC}} \tag{9}$$

$$\mathrm{LSF}(\omega) = \frac{1}{3} + \frac{1}{3}\frac{\theta - \omega}{\theta - \theta_{\mathrm{HPSTC}}} \quad \text{for } \theta_{\mathrm{HPSTC}} < \omega \le \theta \tag{10}$$

where θ is the total meshing angle (i.e. the angular rotation of the driving gear for a complete tooth mesh cycle) and θ_{LPSTC}, θ_{HPSTC} are the meshing angles corresponding to the lowest and highest point of single tooth contact, respectively.

From the above relations it is obvious that according to the AGMA Standard the gear pair starts its engagement with 33% of the total load and the load changes linearly to 67% of the total at the LPSTC. At this point, there is a discontinuous transition to 100% of the load as only one gear pair is in mesh and stays constant until the HPSTC where the load drops again to 67% of the total and changes linearly to 33% until disengagement of the tooth pair. It should be noted that the AGMA standard does not take into account either the individual geometry of the gear teeth or their elastic properties.

The International Standard ISO 6336 [20] gives similar load sharing along the path of contact. The distribution is not perfectly linear during the arcs of approach and recess and it is not symmetrical, although the terminal values of the LSF at critical points of the path of contact, i.e. end-points and HPSTC, LPSTC are exactly the same as those described by the AGMA standard. The governing set of equations is the following (expressed in terms of the meshing angle ω):

$$\mathrm{LSF}(\omega) = \frac{1}{3} + \frac{1}{3}\frac{\tan\omega}{\tan\theta_{\mathrm{LPSTC}}} \quad \text{for } 0 \le \omega < \theta_{\mathrm{LPSTC}} \tag{11}$$

$$\mathrm{LSF}(\omega) = 1 \quad \text{for } \theta_{\mathrm{LPSTC}} \le \omega \le \theta_{\mathrm{HPSTC}} \tag{12}$$

$$\mathrm{LSF}(\omega) = \frac{1}{3} + \frac{1}{3}\frac{\tan\theta - \tan\omega}{\tan\theta - \tan\theta_{\mathrm{HPSTC}}} \quad \text{for } \theta_{\mathrm{HPSTC}} < \omega \le \theta \tag{13}$$

Results and Discussion

The light source for the caustics experimental set-up was a He–Ne laser, equipped with a system of optical filters and lenses to produce the required convergent beam. The specimens (Figure 2) were segments from standard 20° involute gears with module $m = 20$ mm and $z = 18$ teeth, consisting of four teeth each. These were cut on a CNC machining centre from a $t = 5$ mm thick poly-methyl-methacrylate [(PMMA) Plexiglas; Huifeng Organic Plastic Co., Ltd, Wenzhou, China] sheet, selected for its high elastic modulus and its optically isotropic properties. The specimens were placed on a specially designed fixture allowing fine adjustment of the meshing angle, while at the same time allowing loading up to 2000 N to be exerted using calibrated weights. A screen was placed behind the specimen at a distance $z_o = 3405$ mm from the mid-plane of the specimen, in order to record the transmitted caustics. Throughout the tests, the same magnification factor $\lambda_{\mathrm{m}} = 12.5$ was used with the focal point of the convergent laser beam lying behind of the specimen. The gear specimens and the fixture was designed and constructed at the Laboratory of Machine Elements of the NTUA and the caustics experiments took place in the Laboratory of Strength of Materials of the NTUA which provided the laser optical equipment.

The load-sharing factor was experimentally measured for thirteen different meshing angles covering a complete mesh cycle of a gear tooth pair from first engagement to disengagement. The specimens were clamped on the loading device and were statically loaded with a horizontal force of $P = 55.1$ N mm^{-1} per unit width. As both mating teeth were transparent, the resulting caustics were merged and therefore it was

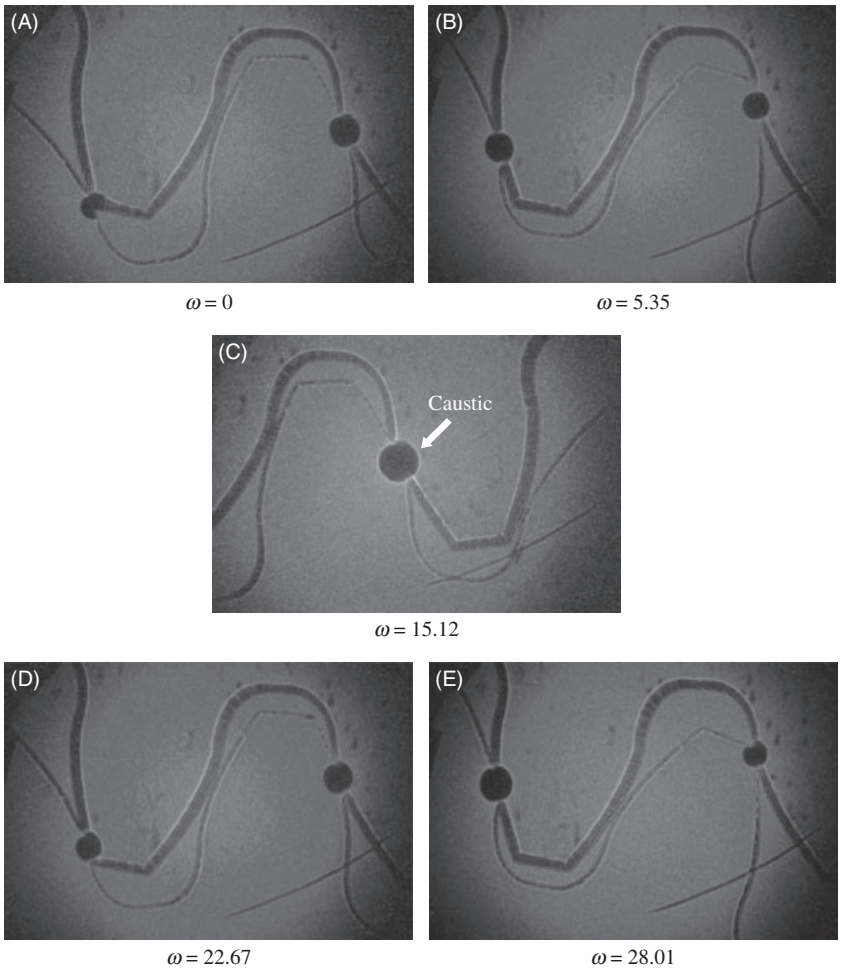

Figure 4A–E: Photographs of transmitted caustics at the contact points for various mesh angles

necessary to cover the mating tooth with a non-transparent material at the point of contact in order to be able to record the geometry of each individual caustic and finally to measure their diameters.

The transmitted caustics are illustrated in Figure 4A–E. In these photographs, taken at consecutive meshing positions, the gradual increase and decrease of the load carried in double tooth contact during approach and recess respectively, as witnessed by the caustics diameters, are evident. The same effect of load variation was verified with planar photoelasticity on 5 mm thick LEXAN polycarbonate specimens of identical geometry, as shown in Figure 5.

From the diameters of the transmitted caustics the load, hence the LSF, was calculated for the different meshing angles from Equations (7) and (4)–(6), using $E = 3400$ MPa, $c_t = -1.55 \times 10^{-4}$ MPa^{-1}, $\nu = 0.34$ for PMMA. The experimentally determined LSF is plotted in Figure 6. The theoretical LSF according to the AGMA and ISO standards are superimposed in the same graph for comparison (solid and dashed lines, respectively).

The experimental results show good agreement with the AGMA and ISO standards, suggesting that the caustics method is a valid tool for experimentally determining the bearing loads and LSF in gear teeth. The observed deviations at the ends of the path of contact can be attributed to the presence of pronounced edge contact and high relative compliance of the used PMMA material to steel, for which the standards were formulated.

Careful sample preparation is essential for obtaining accurate profiles, because typical fine-machining techniques applicable to steel gears cannot be readily applied to PMMA. The maximum manufacturing tooth profile error was kept below 0.04 mm, corresponding to the 0.002 module.

In order to assess the repeatability of the measuring technique, each measurement was repeated several

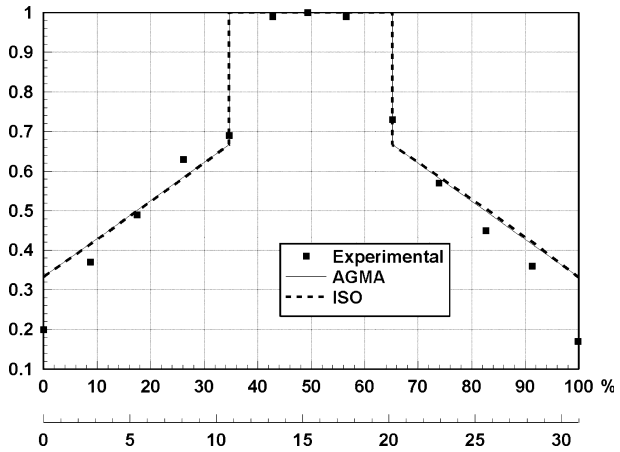

Figure 6: Calculated LSF. Ordinate shown as percentage of mesh cycle and meshing angle

times with intermittent unloading and resetting of the gear positions. Good repeatability was observed, with a maximum deviation <3%. This can be attributed to the close manufacturing tolerances of the loading device and of the specimens and to the good creep resistance of the selected material.

In terms of method efficiency, the calculation of the tooth load involves a single measurement of the maximum caustic diameter, which is automatically processed by means of Equations (7) and (4)–(6). This has been found to be much simpler and expedient than the corresponding photoelastic post processing, which involves computation of path-dependent line integrals, requiring dedicated software tools.

Conclusion

In this paper, the experimental stress-optical method of caustics was applied on meshing gear tooth specimens to determine the load sharing factor during multiple gear tooth contact over a complete meshing

Figure 5: Isochromatic fringe patterns obtained by photoelasticity for double tooth contact (left) and single tooth contact (right)

cycle. The equations of the caustics were used to calculate the magnitude of the applied load at each tooth contact point. The obtained results of the LSF were compared with the pertinent ISO and AGMA standards, with which good agreement was verified.

Furthermore, it was demonstrated that the proposed method has advantages over photoelasticity, because resolution of the measurements is not compromised by the small dimensions of the load-bearing area and the extreme stress gradients observed in it, but instead it is reasonably accurate, highly repeatable and much faster, involving a single measurement of the diameter of the projected caustic. Apart from gears, this technique can be expanded in other applications such as bearings, splines, chains, etc.

REFERENCES

1. Liou C.-H., Lin H., Oswald F. and Townsend D. P. (1996) Effect of contact ratio on spur gear dynamic load. *J. Mech. Design* **118**, 439–443.
2. Munro, R. G. (1988) *Data Item on Profile and Lead Correction*. BGA Technical Publications, Burton, UK.
3. Spitas, C. and Spitas, V. (2006) Calculation of overloads induced by indexing errors in spur gear boxes using multi-degree-of-freedom dynamical simulation. *IMECE J. Multi-Body Dyn.* **220**, 273–282.
4. Cornell, R. W. (1981) Compliance and stress sensitivity of spur gear teeth. *J. Mech. Design* **103**, 447–459.
5. Gosselin, C., Cloutier L. and Nguyen, Q. D. (1995) A general formulation for the calculation of the load sharing and transmission error under load of spiral bevel and hypoid gears. *Mechanism Machine Theory* **30**, 433–450.
6. Zhang Y. and Fang, Z. (1999) Analysis of tooth contact and load distribution of helical gears with crossed axes. *J. Mechanism Machine Theory* **34**, 41–57.
7. Aziz, E. S. and Chassapis, C. (2001) An intelligent system for spur gear design and analysis. Proc. ASME Design Eng. Tech. Conf., 9–12 September, Pittsburg, PA, USA, DETC2001/DAC-21037.
8. Lingaiah, K. and Ramachandra, K. (1977) Three-dimensional photoelastic study of the load carrying capacity/face with ratio of Wildhaber-Novikov gears for automotive applications. *Exp. Mech.* **17**, 392–397.
9. Deuschle, H. M., Wittel, F. K., Gerhard, H., Busse, G. and Kroeplin, B. H. (2006) Investigation of progressive failure in composites by combined simulated and experimental photoelasticity. *Comput. Mater. Sci.* **38**, 1–8.
10. Wang, M. J. (2003) A new photoelastic investigation of the dynamic bending stress of spur gears. *J. Mech. Design* **125**, 365–372.
11. Novikov, A. S., Paikin, A. G., Dorofeyev, V. L., Ananiev, V. M. and Kapelevich, A. L. (2008) Application of gears with asymmetric teeth in turboprop engine gearbox. *Gear Technol.* **January/February**, 60–65.
12. Spitas, V., Costopoulos, T. and Spitas, C. (2006) Optimum gear tooth geometry for minimum fillet stress using BEM and experimental verification with photoelasticity. *J. Mech. Design* **128**, 1159–1164.
13. Spitas, V. and Spitas, C. (2007) Numerical and experimental comparative study of strength-optimzed AGMA and FZG spur gears. *Acta Mech.* **139**, 113–126.
14. Quinn, A. M., Drinkwater, B. W. and Dwyer-Joyce, R. S. (2002) The measurement of contact pressure in machine elements using ultrasound. *Ultrasonics* **39**, 495–502.
15. Manogg, P. (1964) *Anwendung der schattenoptic zur untersuchung des zerreibvorgangs von platen*. Dissertation. University of Freiburg, Germany.
16. Theocaris, P. S. (1970) Local yielding around a crack tip in plexiglass. *J. Appl. Mech.* **92**, 409–415.
17. Theocaris, P. S. and Gdoutos, E. E. (1972) An optical method for determining opening-mode and edge sliding–mode stress intensity factors. *J. Appl. Mech.* **E39**, 91–97.
18. Kalthoff, J. F. (1987) Shadow optical method of caustics. In: *Handbook on Experimental Mechanics*, Chap. 9 (A. S. Kobayashi, Ed.). Prentice Hall, Engelwood Cliffs, New York, 430–500.
19. Papadopoulos, G. (1992) *Fracture Mechanics, The Experimental Method of Caustics and the Det.-Criterion of Fracture*. Springer-Verlag, London.
20. ISO 6336:1996 (1996) *Calculation of the load capacity of spur and helical gears*. ISO.
21. AGMA Standard 2001-B88 (1988) *Fundamental rating factors and calculation methods for involute spur and helical gear teeth*. American Gear Manufacturers Association.
22. Johnson, K. L. (2001) *Contact Mechanics*. Cambridge University Press, United Kingdom.
23. Sfantos, G., Spitas V. and Costopoulos, T. (2003) Analytical and experimental study of bearing stresses developed on machine elements in contact. NTUA, Dept. Mech. Eng., Lab. Machine Elements, No. TR-SM-0302, February.
24. Papadopoulos, G. A. (2005) Experimental study of the load distribution in bearings by the method of caustics and the photoelasticity method. *Strain Anal. Eng. Design* **40**, 357–366.

